AIP Journal of Applied Physics

Computer simulation of electron beams. II. Low-cost beam-current reconstruction

D. A. de Wolf

Citation: Journal of Applied Physics **58**, 3697 (1985); doi: 10.1063/1.335631
View online: http://dx.doi.org/10.1063/1.335631
View Table of Contents: http://scitation.aip.org/content/aip/journal/jap/58/10?ver=pdfcov
Published by the AIP Publishing

Computer simulation of electron beams. II. Low-cost beam-current reconstruction

D. A. de Wolf[a)]
Department of Electrical Engineering, Virginia Polytechnic Institute and State University, Blacksburg, Virginia 24061

(Received 1 July 1985; accepted for publication 1 August 1985)

Reconstruction of current density in electron beams is complicated by distortion of phase space which can require very fine discretization of the beam into trajectories. An efficient discretization of phase space is exploited, using conservation of charge and current in hypertriangle patches, to reconstruct the current density by fitting Gaussians through the distorted hypertriangles. Advantages and limitations are discussed.

I. INTRODUCTION

Thin quasilaminar electron beams (e.g., as in kinescope drift regions) can be simulated by computer accurately and efficiently by neglecting longitudinal space-charge forces.[1] Not many beamlet trajectories are required to compute accurately the phase-space coordinates q_x, p_x, q_y, p_y, p_z in some equipotential plane. However, the reconstruction of the beam current density is entirely another matter. A poor choice of beamlets (into which the beam is discretized) can lead to a poor beam-current representation, no matter how large the number of beamlets. An example is shown in Fig. 1; a circular source of electrons is focused into a smaller circular spot at $z = L$. If only three directions of the initial beam are chosen in discretization (as in the lower half of the figure), the focal spot will also consist of three discrete pieces; obviously the ensuing current-density distribution is unrealistic even though a continuum of electrons are simulated in each of the three directions.

In this paper, we show that beam discretization must be linked to that of the single-particle phase-space density function $f(\mathbf{q},\mathbf{p})$ in order to avoid inaccuracies as described above. The four- (or five-) dimensional function $f(\mathbf{q},\mathbf{p})$ is simulated by a sum of Gaussians in the same number of dimensions, each of which is essentially nonzero in only a small part of phase space. The restriction on size of these Gaussian patches is dictated by the requirement that coordinate and momentum differences with a central reference trajectory in each path transform as linear functions of the initial differences as the beam propagates. That ensures that Gaussians remain Gaussians. As a result it is possible to integrate over momentum space analytically to obtain contributions to current density which are then summed to yield $j(\mathbf{q})$. In the presented algorithm, the constants of each Gaussian are determined by fitting moments to those of the actual distribution as determined by a minimum set of key trajectories (five in four dimensions).

We present comparisons with current-density distributions determined accurately by Monte Carlo methods for axisymmetric beams. No use is made of the axial symmetry in the algorithm so that magnetically deflected beams can be simulated. However, comparisons of asymmetric deflected beams calculated as above with laboratory simulations will be deferred to future work. Initial comparisons show qualitatively correct behavior.

II. THEORY

A beam of electrons in a static electromagnetic field including space charge can be described by a six-dimensional phase space density $f_d(\mathbf{q},\mathbf{p})$ where $\mathbf{p}$ is the momentum of an electron at location $\mathbf{q}$.[2] The coordinate system is so chosen that q_3, p_3 correspond to the trajectory tangent direction of a reference electron at any location. Phase-space conservation[3,4] yields

$$d^3Qd^3P = d^3qd^3p,$$
$$F_d(\mathbf{Q},\mathbf{P}) = f_d(\mathbf{q},\mathbf{p}), \tag{1}$$

if point $(\mathbf{q},\mathbf{p})$ in phase space transforms into $(\mathbf{Q},\mathbf{P})$ by electron motion. One degree of freedom is removed if $q_3 = \text{const}$ and $Q_3 = \text{const}$ are both equipotential planes. Consequently, the current density at $Q_3 = \text{const}$ is given by

$$j(\mathbf{Q}_T) = \frac{1}{m}\int\int\int d^2P_T dP_3 P_3 F_d(\mathbf{Q}_T, P_T, p_3), \tag{2}$$

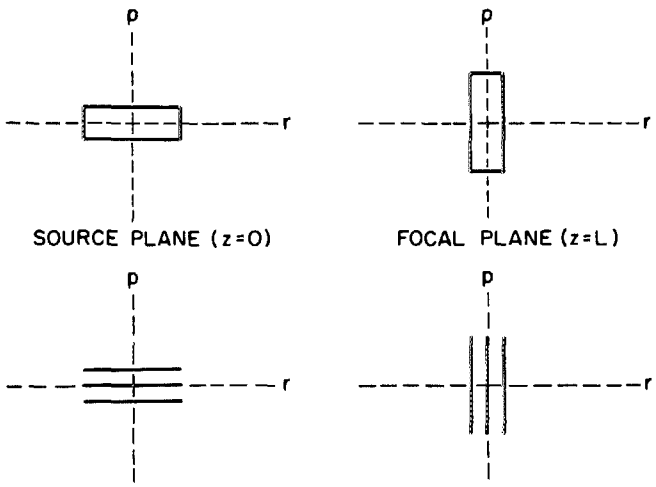

FIG. 1. Perfect focus of a circular beam with limited angles of emission: phase space of radial r and p (above), and for discretized beam (below).

[a)] This work was performed while the author was still at RCA Laboratories, Princeton, NJ 08540.

 0021-8979/85/223697-06$02.40

where subindex T refers to the transverse coordinates. The motion of an electron in the packet represented by Eq. (2) is governed by the single-particle Hamiltonian,

$$H(\mathbf{q},\mathbf{p}) = p^2/2m - e\Phi(\mathbf{q}), \tag{3}$$

where e and m are the electron charge and mass, respectively, and $\Phi(\mathbf{q})$ is the electrostatic potential (which may include space-charge forces). $H(\mathbf{q},\mathbf{p})$ is conserved along each trajectory, hence,

$$\mathbf{P}_T^2 + P_3^2 = 2em[\Phi(\mathbf{Q}_T) - \Phi(\mathbf{q}_T)] + \mathbf{p}_T^2 + p_3^2. \tag{4}$$

The differential dP_3 in Eq. (2) can be approximated (see Appendix A) by

$$dP_3 \approx (p_3/P_3)dp_3 \tag{5}$$

when chromatic aberrations are negligible in the transverse coordinates $\mathbf{Q}_T,\mathbf{P}_T$. A useful choice of the coordinates $\mathbf{Q}_T$, $\mathbf{P}_T,P_3$ is such that P_3 is tangential at the $Q_3 = \text{const}$ plane to a central reference trajectory of the beam. For quasilaminar beams (i.e., beams in which electron trajectories cross mostly at very small angles to each other) it follows that $P_T \ll P_3$ everywhere except in the immediate vicinity of the source. Therefore, the term $\mathbf{P}_T^2$ in Eq. (4) can be neglected almost everywhere, and because $(p_T^2 + p_3^2)/2m \ll e[\Phi(\mathbf{Q}_T) - \Phi(\mathbf{q}_T)]$[5] it also follows that $(p_T^2 + p_3^2) \ll P_3^2$. From this and from Eq. (5) it can be observed that $dP_3 \ll P_3$ almost everywhere, so that for all practical purposes the density function $F_d(\mathbf{Q}_T,\mathbf{P}_T,p_3)$ is sharply peaked around a value of $P_3 = \bar{P}_3$ with

$$\bar{P}_3^2 = 2em[\Phi(\mathbf{Q}_T) - \Phi(\mathbf{q}_T)] + \bar{p}_3^2, \tag{6}$$

where $\bar{p}_3$ is a (yet to be defined) average value of p_3. In fact F_d can then be approximated by

$$F_d(\mathbf{Q}_T,\mathbf{P}_T,p_3) = \bar{F}_d(\mathbf{Q}_T,\mathbf{P}_T)\delta(p_3 - \bar{p}_3). \tag{7}$$

Equations (5)–(7) indicate that the situation at $Q_3 = \text{const}$ is not appreciably altered if f_d is approximated by

$$f_d(\mathbf{q}_T,\mathbf{p}_T,p_3) = \bar{f}_d(\mathbf{q}_T,\mathbf{p}_T)\delta(p_3 - \bar{p}_3). \tag{8}$$

The average longitudinal momentum $\bar{p}_3$ and the transverse phase-space density $\bar{f}_d(\mathbf{q}_T,\mathbf{p}_T)$ are inferred from

$$j(\mathbf{q}_T) = \frac{1}{m}\int d^2p_T \int_0^\infty dp_3\, p_3 f_d(\mathbf{q}_T,\mathbf{p}_T,p_3)$$

$$= \frac{1}{m}\int d^2p_T\, \bar{p}_3 \bar{f}_d(\mathbf{q}_T,\mathbf{p}_T). \tag{9}$$

Finally, we substitute $F_d(\mathbf{Q}_T,\mathbf{P}_T,p_3) = f_d(\mathbf{q}_T,\mathbf{p}_T,p_3) = \bar{f}_d(\mathbf{q}_T,\mathbf{p}_T)\delta(p_3 - \bar{p}_3)$ into Eq. (2) and use Eq. (5) to replace P_3dP_3 by p_3dp_3 to obtain

$$j(\mathbf{Q}_T) = \frac{1}{m}\iint d^2P_T f_c(\mathbf{q}_T,\mathbf{p}_T), \tag{10}$$

where $f_c(\mathbf{q}_T,\mathbf{p}_T) \equiv \bar{p}_3 f_d(\mathbf{q}_T,\mathbf{p}_T)$ is the four-dimensional *current* density at the source. At fixed values of $p_3 = \bar{p}_3, P_3 = \bar{P}_3$, the trajectory coordinates $\mathbf{q}_T,\mathbf{p}_T$ transform into $\mathbf{Q}_T,\mathbf{P}_T$. In general, the transformation is quite nonlinear, e.g., as depicted in Fig. 4 for a symmetric kinescope beam focused onto a screen. Hence, even for a typical cathode density of relatively simple form,[6]

$$f_c(\mathbf{q}_T,\mathbf{p}_T) = j_0(1 - q_T^2/R_0^2)^{3/2}\frac{1}{2\pi mkT}e^{-p_T^2/mkT}, \tag{11}$$

rather complicated forms of $F_c(\mathbf{Q}_T,\mathbf{P}_T)$ ensue upon replacing $\mathbf{q}_T$ and $\mathbf{p}_T$ by their (inverse) functional dependence upon $\mathbf{Q}_T,\mathbf{P}_T$ in $f_c(\mathbf{q}_T,\mathbf{p}_T)$. On the other hand, numerical integration of the transverse momenta in

$$j(\mathbf{Q}_T) = \frac{1}{m}\iint d^2P_T F_c(\mathbf{Q}_T,\mathbf{P}_T) \tag{12}$$

is also fraught with difficulties because, as exemplified in Fig. 4, the boundaries of d^2P_T are very difficult to ascertain: Many well-chosen trajectories are needed to adequately fill in the transverse phase-space area.

III. GAUSSIAN DECOMPOSITION OF PHASE SPACE

The idea behind Gaussian decomposition is to replace the transverse phase-space current density $f_c(\mathbf{q}_T,\mathbf{p}_T)$ by a sum of Gaussians,

$$\bar{f}_c(\mathbf{x}^4) = \sum_i \kappa^{(i)} \exp\left(-\sum_{m,n=1}^{4}\alpha_{mn}^{(i)}[x_m - \bar{x}_n^{(i)}][x_n - \bar{x}_n^{(i)}]\right), \tag{13}$$

where $\mathbf{x}^4 = (x_1,x_2,x_3,x_4)$ is a convenient notation for the four-vector (q_1,p_1,q_2,p_2). Each Gaussian (indicated by summation index i) is characterized by four center coordinates $\bar{x}_m^{(i)}$, ten quadratic coefficients $\alpha_{mn}^{(i)}$ (with $\alpha_{nm}^{(i)} = \alpha_{mn}^{(i)}$), and a normalizer $\kappa^{(i)}$: fifteen constants in total per Gaussian. It is crucial to our methods that the $\alpha_{mn}^{(i)}$ restrict essentially nonzero values of the Gaussian to a small "patch" in 4D space around the four-vector $\bar{x}^4 = [\bar{x}_1^{(i)},\bar{x}_2^{(i)},\bar{x}_3^{(i)},\bar{x}_4^{(i)}]$ such that the transformation from q_3 to Q_3 defines a linear transformation,

$$X_m - \bar{X}_m^{(i)} = \sum_{m=1}^{4} T_{mn}^{(i)}[x_n - \bar{x}_n^{(i)}], \tag{14}$$

where $\bar{x}^4$ transforms into $\bar{X}^4 = [\bar{X}_1^{(i)},\ldots,\bar{X}_4^{(i)}]$. The 4 by 4 matrix $\mathbb{T}$ with coefficients $T_{mn}^{(i)}$ is the Jacobian of the transformation $d^2q_Td^2p_T$ to $d^2Q_Td^2P_T$ and it can be determined thus in principle (see later). Let A be a 4 by 4 matrix with coefficients $\alpha_{mn}^{(i)}$. It follows that Eq. (13) can be rewritten as

$$\bar{f}_c(\mathbf{x}^4) = \sum_i \kappa^{(i)} \times \exp\left(-\sum_{m,n=1}^{4}\bar{\alpha}_{mn}^{(i)}[X_m - \bar{X}_m^{(i)}][X_n - \bar{X}_n^{(i)}]\right)$$

$$\equiv \bar{F}_c(X^4), \tag{15}$$

$$\bar{\alpha}_{mn}^{(i)} = [(\mathbb{T}^{-1})^T \cdot \mathsf{A} \cdot (\mathbb{T}^{-1})]_{mn}.$$

Substitution of Eq. (15) into Eq. (10), under the assumption that $\bar{f}_c(\mathbf{x}^4)$ is a good representation of $f_c(\mathbf{x}^4)$, leads to a sum of analytically tractable integrals:

$$j(X_1,X_3) \approx \sum_i \kappa^{(i)} \int_{-\infty}^{\infty}\int dX_2dX_4 \times \exp\left(-\sum_{m,n=1}\bar{\alpha}_{mn}^{(i)}[X_m - \bar{X}_m^{(i)}][X_n - \bar{X}_n^{(i)}]\right)$$

$$= \sum_i \kappa^{(i)}\Lambda^{(i)} \times \exp(-\gamma_{11}^{(i)}\delta X_1^2 - 2\gamma_{13}^{(i)}\delta X_1\delta X_3 - \gamma_{33}\delta X_3^2),$$

$$\delta X_1 \equiv X_1 - X_1^{(i)}, \tag{16}$$

$$\delta X_3 \equiv X_3 - X_3^{(i)}.$$

The new constants, $\Lambda^{(i)}$, $\gamma_{11}^{(i)}$, $\gamma_{13}^{(i)}$, $\gamma_{33}^{(i)}$ are easily evaluated as functions of $\alpha_{mn}^{(i)}$ (we need not specify them here).

To summarize the differences: A straightforward calculation of $j(\mathbf{Q}_T)$ via Eq. (12) is difficult because the transformed phase space occupied by the beam is very distorted and because even a very large selection of beamlets at the source does not guarantee a uniformly filled phase space after beam propagation. The Gaussian decomposition replaces beamlets by a hopefully much smaller sum of four-dimensional Gaussians which do fill phase space uniformly. The numerical price to be paid is that 15 constants per Gaussian must be determined, and that $\bar{f}_c(\mathbf{x}^4)$ as given by Eqs. (13) must be a reasonable representation of $f_c(\mathbf{x}^4)$, e.g., as given by Eq. (11).

IV. NUMERICAL COMPUTATION: COARSE MOMENTUM DISCRETIZATION

The ability to reproduce a beam current-density profile of a beam cross section depends strongly on how well $f_c(\mathbf{x}^4)$ is represented by a sum of Gaussians $\bar{f}_c(\mathbf{x}^4)$ in four-dimensional phase space. Because the index i in Eq. (13) must range over four dimensions, the total number of Gaussians can easily grow to be unmanageable.

Experience with axisymmetric beams in kinescopes[7-9] (for which the azimuthal symmetry greatly reduces the number of electron beamlets) has shown that a very coarse discretization of momentum space suffices.[7] This will be exploited in a scheme that will be illustrated by a simulation of a kinescope beam with source-current phase-space density given by Eq. (11). The present scheme does not utilize axial symmetry, although the illustrative examples to be discussed are all axisymmetric.

In order to calculate the coefficients $\alpha_{mn}^{(i)}$ we attempt to fit Gaussians through the "hypertriangles" in 4D space with five vertices that consist of three chosen from many equilateral triangles in coordinate subspace (Fig. 2) filling the region where $q_T < R_0$ [in Eq. (11)], and of two chosen from only one equilateral triangle in momentum subspace [vertices of which correspond to the $1/e$ values of the exponential in Eq. (11)]. The $P_T = 0$ trajectories are launched from the vertices and the three $P_T \neq 0$ trajectories from the centers of the discretization triangles in coordinate subspace. Each hypertriangle consists of three $\mathbf{p}_T = 0$ and two $\mathbf{p}_T \neq 0$ beamlets launched from one equilateral triangle inside $|\mathbf{q}_T| = R_0$. While 4D space is covered rather cursorily in this fashion, we do in some physical sense represent cathode emission everywhere in a number of important directions. Each beamlet is then given a portion of current, weighted by Eq. (11), so that each triangle and hypertriangle carry the correct amount of current.

The moments of Eq. (13) are

$$\langle x_1^m x_2^n x_3^p x_4^q \rangle = \int d^4x x_1^m x_2^n x_3^p x_4^q \bar{f}_c(\mathbf{x}^4) \Big/ \int d^4x \bar{f}_c(\mathbf{x}^4). \quad (17)$$

The numerator of Eq. (17), for $m = n = p = q = 0$ represents the total current emitted by a hypertriangle (equals 1/3 of the current emitted by a triangle of Fig. 2(a) in the present scheme), and thus allows $\kappa^{(i)}$ to be determined. The $\alpha_{mn}^{(i)}$ are determined by the second moments $m + n + p + q = 2$, and

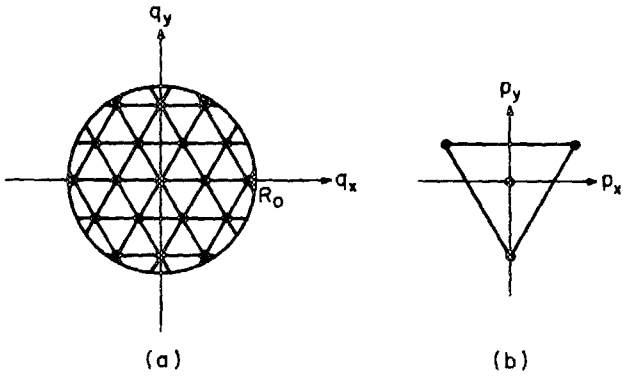

FIG. 2. Discretization of phase space into hypertriangles: coordinate part (a) and momentum part (b).

the $\bar{x}_m^{(i)}$ follow from the first moments $m + n + p + q = 1$. These moments are equated to those of the discretized beamlets.

A trivial application of the algorithm is shown in Fig. 3 at $Q_3 = q_3 = \text{const}$ for the curve

$$j(\mathbf{q}_T) = j_0(1 - q_T^2/R_0^2)^{3/2}, \quad (18)$$

for $R_0 = 8.1$ mils and a convenient (but not relevant) value of the constant j_0. Curve (18) is shown as a heavy solid line. Let h be the length of a side of a triangle. The remaining three curves in Fig. 3 show calculations of $j(\mathbf{q}_T)$ via the algorithm in three radial directions for $h = 1$ mil (i.e., for almost 1200 hypertriangles in four space). Because the Gaussian exponential constants are obtained by fitting moments, and because Eq. (11) determines a relatively smooth and slowly varying spatial dependence of $f_T(\mathbf{q}_T, \mathbf{p}_T)$ upon q_1 and q_2, the ensuing Gaussian functions are somewhat narrow (and strongly peaked) per interval $\delta q_T = h$, thus giving rise to strong oscillations in reconstruction of $j(\mathbf{q}_T)$. These oscilla-

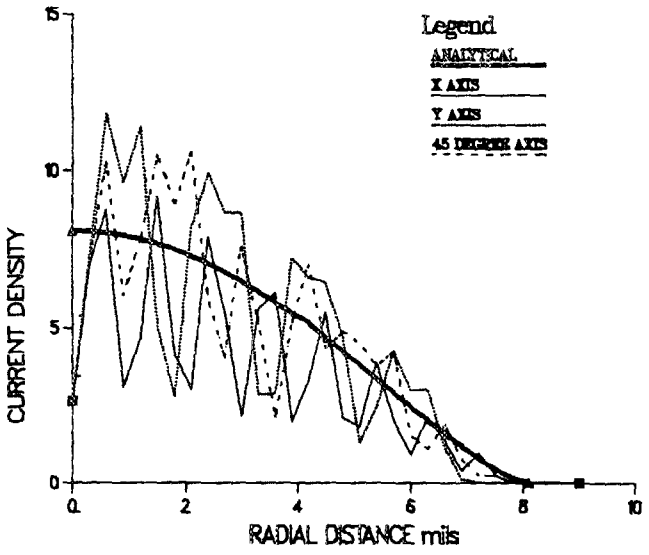

FIG. 3. Reconstruction of current density of Eq. (18) with Gaussian decomposition of phase space.

TABLE I. Two sets of parameter values for Eq. (19).

	θ_0	α_1	α_2	α_3	β	γ	Λ	Figures	Type of Spot
A	35°	0.030	0.030	0	1.5	2.5	45	4,5	almost focused
B	24°	0.027	0.027	0	0.5	2.8	50	6,7	underfocused

tions can be suppressed by choosing other methods of fitting Gaussians through $f_c(\mathbf{q}_T,\mathbf{p}_T)$.[10] They are not important here because the algorithm is to be applied to highly distorted phase spaces in which the two-dimensional projections of the Gaussians tend to overlap and smooth out the oscillations.

The phase space of a beam emitted from a thermionic cathode and electron optically focused onto a screen, e.g., as in cathode-ray tubes, has a familiar rotated and distorted shape.[11] In order to simulate a realistic situation by Monte Carlo methods of tracing electrons from cathode to screen at nonprohibitive computer-time cost, the following transformation was used,

$$\begin{bmatrix} Q_1 \\ P_1 \\ Q_2 \\ P_2 \end{bmatrix} = \begin{bmatrix} 1 & \Lambda & 0 & 0 \\ 0 & 1 & 0 & 0 \\ 0 & 0 & 1 & \Lambda \\ 0 & 0 & 0 & 1 \end{bmatrix} \begin{bmatrix} -\beta \sin\theta & \gamma \cos\theta & 0 & 0 \\ -\gamma^{-1}\cos\theta & -\beta^{-1}\sin\theta & 0 & 0 \\ 0 & 0 & -\beta\sin\theta & \gamma\cos\theta \\ 0 & 0 & -\gamma^{-1}\cos\theta & -\beta^{-1}\sin\theta \end{bmatrix} \begin{bmatrix} q_1 \\ p_1 \\ q_2 \\ p_2 \end{bmatrix}, \tag{19}$$

$$\theta = \theta_0 + \alpha_1(q_1^2 + \beta^{-2}\gamma^2 p_1^2) + \alpha_2(q_2^2 + \beta^{-2}\gamma^2 p_2^2) + \alpha_3(q_1 p_2 - q_2 p_1).$$

Table I gives two useful choices of the parameters. The procedure outlined in connection with Fig. 2 has been followed to discretize the density distribution (11) with $h = 1$ mil and $R_0 = 8.1$ mils. This leads to nearly 1600 beamlets which in turn yield scatter plots representing typical distorted phase spaces of almost-focused spots (A) in Fig. 4 and well-underfocused spots (B) in Fig. 6 after application of Eq. (19) to the discretized $\mathbf{q}_T,\mathbf{p}_T$ coordinates. The hypertriangle + Gaussian-fitting procedure then yields $j(\mathbf{Q}_T)$ vs $\mathbf{Q}_T$ curves in three radial directions for case A in Fig. 5 and for case B in Fig. 7. The heavy solid curves in Figs. 5 and 7 are obtained from a Monte Carlo simulation of $j(\mathbf{Q}_T)$ with Eq. (19) by selecting 60 000 pairs q_T, p_t (utilizing azimuthal symmetry) from the density distribution (11). The Monte Carlo curves are accurate to within a few percent except in the immediate vicinity of $q_T = 0$.

The comparison indicates that the distortion of phase space has indeed smoothed out the undulations present in Fig. 3, and reasonable agreement is found in spite of the coarseness of the discretization of the two momentum dimensions of phase space.

V. COMMENTS ON ACCURACY VERSUS EFFICIENCY

The stress in developing a numerical algorithm has been on efficiency, because many beams need to be analyzed and high accuracy is not required for design purposes. One problem with respect to keeping computer time within reasonable limits lies in the fact that the number of hypertriangles is proportional to h^{-4} (if h is the length of a side of one hypertriangle). The advantage of a coarse discretization of the momentum subspace, e.g., as in Fig. 2(b), lies in the less rapid increase of the number of hypertriangles to be fitted by Gaussians h^{-2} (as h is decreased). The numerical examples discussed above, as well as a number of other more realistic test cases not discussed here, show rapid convergence in $j(\mathbf{q}_T)$ as the parameter R_0/h increases above a value of the

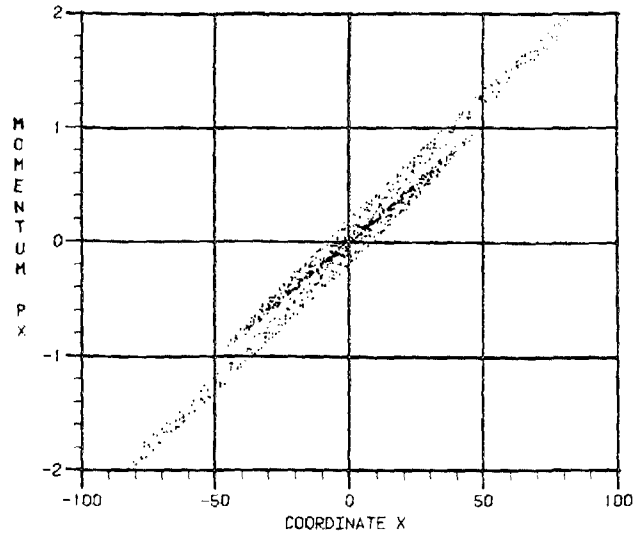

FIG. 4. Phase space p_x vs x of Eq. (19) with choice A of Table I.

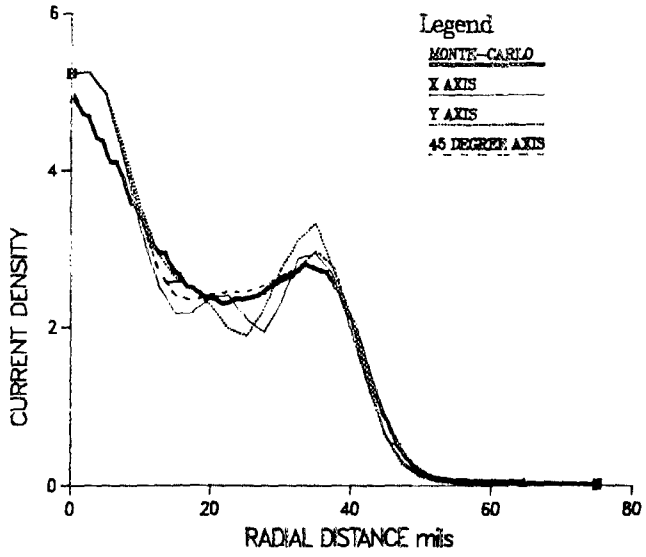

FIG. 5. Reconstruction of current density (in arbitrary units) of Eq. (19) for choice A of Table I.

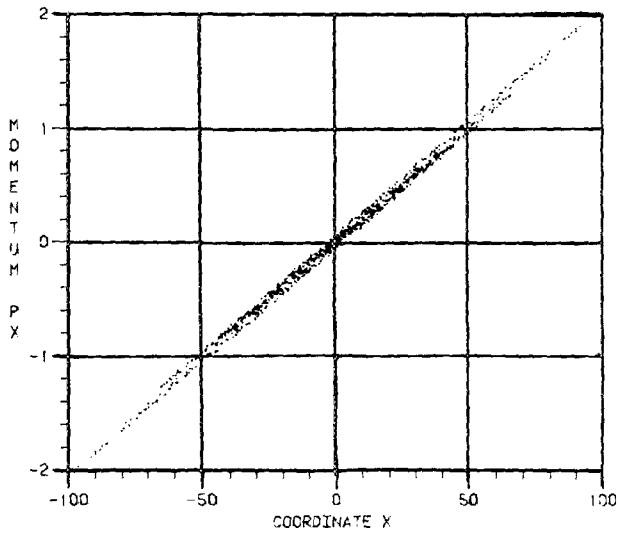

FIG. 6. Phase space p_x vs x of Eq. (19) with choice B of Table I.

order of $R_0/h = 6$. The remaining discrepancies with analytical (or measured) results must therefore be due to the coarseness of the momentum-subspace discretization.

As momentum subspace is discretized more finely, the number of hypertriangles grows, but the difficulty of this method is enhanced even more so by the fact that the bookkeeping of all possible hypertriangles becomes very complicated. Other methods of calculating $\bar{\alpha}^{(l)}_{mn}$, that circumvent this difficulty, exist[12] but there is a numerical price to be paid in discretizing momentum space more finely.

However, the Gaussian-fitting method was devised to reconstruct beams that are simulated numerically with space-charge forces and (magnetic) deflection. The need to obtain spatial fields at many points along a trajectory, even with an efficient space-charge algorithm,[1] makes it desirable to keep the number of trajectories as small as possible. Coarse discretization of momentum subspace is therefore a significant advantage, even though some decrease in accuracy results. It is apparent from the numerical examples, as well as from many other beam simulations not presented here, that reasonable beam current reconstructions can thus be obtained. That is a significant advantage in the evaluation of electron-optics devices such as cathode-ray tubes, kinescopes, etc.

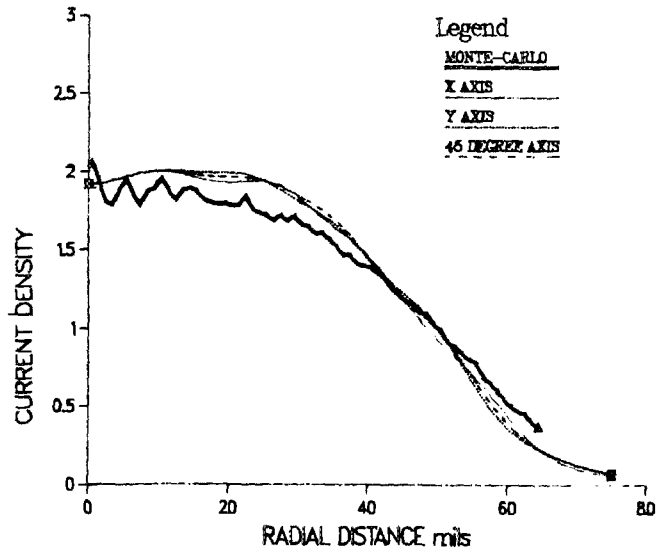

FIG. 7. Reconstruction of current density (in arbitrary units) of Eq. (19) for choice B of Table I.

ACKNOWLEDGMENT

This work has benefitted greatly from stimulating discussions with C. H. Anderson, A. Pelios, J. R. Fields, and other workers in electron optics at RCA Laboratories.

APPENDIX A: VARIATION OF P_3 (REF. 14)

Let $(X_1,X_2,X_3,X_4) = (Q_1,P_1,Q_2,P_2)$ and likewise let $(x_1,x_2,x_3,x_4) = (q_1,p_1,q_2,p_2)$. The variation of P_3 such that there is no concomitant variation in X_1, X_2, X_3, and X_4 is

$$(dP_3)_X = (\partial P_3/\partial p_3)_X (dp_3)_X + \sum_{i=1}^{4} (\partial P_3/\partial x_i)_{p_3} (dx_i)_X. \quad \text{(A1)}$$

The four variations $(dx_i)_X$ are not independent because

$$0 = dX_i = (\partial X_i/\partial p_3)_x (dp_3)_X + \sum_{j=1}^{4} (\partial X_i/\partial x_j)_{p_3} (dx_j)_X, \quad \text{(A2)}$$

for $1 \leqslant i \leqslant 4$. Let $T_{ij} = (\partial X_i/\partial x_j)_{p_3}$ be the ij element of the transverse Jacobian matrix T of the transform between d^4X_i and d^4X_i, i.e.,

$$(d^4X)_{P_3} = \det|\mathsf{T}| \cdot (d^4x)_{p_3}. \quad \text{(A3)}$$

It follows from Eq. (A2) that

$$(dx_i)_X = -\sum_{j=1}^{4} (\mathsf{T}^{-1})_{ij} (\partial X_j/\partial p_3)_X (dp_3)_X, \quad \text{(A4)}$$

and therefore from Eqs. (A4) and (A1) that

$$(dP_3)_X = \left[(\partial P_3/\partial p_3)_x - \sum_{i,j=1}^{4} (\partial P_3/\partial x_i)_{p_3} \times (\mathsf{T}^{-1})_{ij} (\partial X_j/\partial p_3)_x \right] (dp_3)_X. \quad \text{(A5)}$$

The first term in the square brackets is p_3/P_3, according to Eq. (4). The second group of terms can be shown to be quite small compared to p_3/P_3 by considering the equations of motion,[13]

$$\mathbf{Q}_T = \mathbf{q}_T + \int_0^s ds_1 \mathbf{p}_T(s_1) / \left[p_T^2(s_1) + p_3^2(s_1) \right], \quad \text{(A6)}$$

$$\mathbf{P}_T = \mathbf{p}_T - em \int_0^s ds_1 \frac{\partial \Phi}{\partial \mathbf{q}_T(s_1)} \Big/ \left[p_T^2(s_1) + p_3^2(s_1) \right].$$

Except close to $s_1 = 0$ (s_1 is the ray coordinate) it follows from Eq. (4) that the denominators in Eq. (A6) are almost entirely determined by the potential differences at s_1 and at 0 so that $\mathbf{Q}_T$ and $\mathbf{P}_T$ are only very slightly influenced by $p_3(0) = p_3$. Therefore $(\partial X_j/\partial p_3)_x$ is very small, and in practice sufficiently small to enable one to ignore chromatic aberrations. As a result,

$$(dP_3)_x \approx (\partial P_3/\partial p_3)_x (dp_3)_X \approx (p_3/P_3)(dp_3)_X. \quad \text{(A7)}$$

[1] D. A. de Wolf, J. Appl. Phys. **58**, 3692 (1985).

[2] C. Lejeune and J. Aubert, in *Advances in Electronics and Electron Physics*,

Supplement BA, edited by A. Septier (Academic, New York, 1980), p. 159.
[3]A. L. Lichtenberg, *Phase-Space Dynamics of Particles* (Wiley, New York, 1969).
[4]J. D. Lawson, *The Physics of Charged-Particle Beams* (Clarendon, Oxford, 1977).
[5]The momentum distribution at the source is usually governed by a Boltzmann factor $\exp[-(p_T^2+p_3^2)/2mkT]$, where $kT \ll |e|\Phi(\mathbf{Q}_T)$ at almost all locations away from the source.
[6]The constant j_0 in Eq. (11) can be expressed as $j_0 = 5I/2\pi R_0^2$, where I is the total beam current. We will regard j_0 as an unspecified constant.
[7]F. J. Campbell (private communication); also R. H. Hughes and H. Y. Chen, IEEE Consumer Electron. **CE-25**, 185 (1979).
[8]C. Weber, Philips Technol. Rev. **24**, 130 (1962).
[9]D. L. Say, R. B. Jaeger, and J. D. Ryan, IEEE Trans. Consumer Electron. **CE-21**, 56 (1975).
[10]R. Sverdlove and R. W. Klopfenstein (private communication).
[11]S. Washino, Y. Ueyama, and S. Takenobu, IEEE Trans. Consumer Electron. **CE-25**, 481 (1979).
[12]N. D. Winarsky and R. Sverdlove (private communication).
[13]Chen Yin-bao and Yie Xi, IEEE Trans. Nucl. Sci. **NS-28**, 2500 (1981).
[14]Much of the ensuing derivation follows an argument provided by J. R. Fields.